Unmanned Systems, Vol. 14, No. 4 (2026) 839–852

DOI: 10.1142/S2301385026500226

UNMANNED SYSTEMS
https://www.worldscientific.com/worldscinet/us

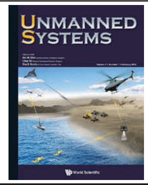

Cooperative Guidance Law Considering Tangential Acceleration Constraint

Xiaofei Dong*,†,§, Zhang Ren*, Jinwen Hu‡

*School of Automation Science and Electrical Engineering,
Beihang University, Beijing 100191, P. R. China

†National Key Laboratory of Complex System Control and Intelligent Agent Cooperation,
Beijing 100074, P. R. China

‡School of Automation, Northwestern Polytechnical University,
Xi'an 710072, P. R. China

A novel finite-time cooperative guidance (FnTCG) law is proposed in this paper for multi-aircraft systems to achieve cooperative attacks on maneuvering targets with three-dimensional LOS angle control. The FnTCG law employs tangential acceleration for salvo attacks along the LOS direction and normal acceleration for terminal angle-constrained interceptions. The methodology comprises three key steps. First, a finite-time extended state observer is designed to estimate the target-induced disturbances. Second, using the finite-time observer and consensus protocol, normal accelerations are developed to converge the LOS angles to the desired values within a finite time. Finally, a consensus protocol is used to derive the tangential acceleration under input constraints to ensure finite-time salvo attacks. Notably, this work avoids linearization, eliminates singularity issues, and enables input saturation. The finite-time stability of the proposed FnTCG law is rigorously established. Numerical simulations demonstrate its effectiveness and advantages in comparison to existing methods.

Keywords: Cooperative guidance; maneuvering targets; salvo attack.

1. Introduction

Cooperative guidance has received significant attention owing to its potential to enhance mission success rates, target neutralization efficiency, and interception accuracy in engagements against maneuvering targets. Early research primarily focused on impact time control guidance (ITCG) and impact angle control guidance (IACG) [1–4], where each aircraft independently controls its speed and acceleration with no inter-coupling relationships. These implicit cooperative guidance methods require presetting the desired impact time and impact angle parameters for each aircraft before launch, which is often complicated by numerous influencing variables. Unreasonable parameters can result in excessive energy consumption and even cause mission failure.

To overcome the drawbacks of the implicit cooperative guidance law, many researchers have devoted their efforts to establishing an explicit cooperative guidance law. Chen *et al.* [5] developed a two-stage cooperative guidance framework. In the first stage, consensus algorithms and feedback linearization are employed to synchronize the remaining flight time across multiple aircraft, while the second stage utilizes proportional navigation to address singularity challenges inherent in cooperative guidance systems. Sinha *et al.* [6] developed a novel cooperative guidance law based on sliding mode control and event-triggering strategies. This approach ensures simultaneous impacts by multiple aircraft while reducing the frequency of guidance strategy triggers, which reduces the computational loads. Furthermore, in the realm of leaderless distributed cooperative guidance for fixed targets, researchers have explored various aspects, including constraints on the field-of-view angle,

Received 28 October 2024; Revised 3 March 2025; Accepted 4 March 2025; Published 18 June 2025. This paper was recommended for publication in its revised form by editorial board member, Radhakant Padhi.
Email Address: §dxf891112@126.com
§Corresponding author.

fault-tolerant strategies, communication topology, and finite-time convergence. Dong *et al.* [7] presented a distributed three-dimensional cooperative guidance law for multiple aircraft with seeker field-of-view angle constraints. This guidance law builds on the proportional navigation approach by incorporating a biased term to regulate the remaining flight time. The bias term consists of two auxiliary functions to ensure that the guidance law remains nonsingular and complies with the field-of-view angle constraints. This innovation enables the guidance law to tackle issues related to guidance command switching in multi-stage strategies. Addressing the impact angle constraints, Wang *et al.* [8] investigated scenarios involving simultaneous attacks with a constant aircraft speed. They developed distributed cooperative guidance laws for both single-plane and three-dimensional contexts. By introducing auxiliary functions, they effectively managed singularity problems while ensuring fixed-time convergent stability. Zhang *et al.* [9] delved into the challenge of optimal distributed three-dimensional cooperative guidance for multiple interceptors that target stationary objects under directed topology conditions. They proposed a two-stage cooperative guidance law, which incorporated an optimal consensus method with fixed-time convergence in the first stage. This method ensures uniform remaining flight time among multiple aircraft, regardless of the initial conditions. In the second stage, pure proportional navigation facilitates saturation attacks on the target. Therefore, the cooperative guidance law proposed in this paper effectively avoids singularities while ensuring that the tangential acceleration along the LOS satisfies the input saturation constraints. Cooperative guidance laws are designed against stationary targets and cannot be applied to maneuvering targets.

Cooperative guidance law against maneuvering targets is of practical importance but more difficult to design than that against a stationary target. Shaferman and Shima [10, 11] initially explored the interception of maneuvering targets by multiple aircraft. They developed cooperative guidance laws based on optimal control methods. Their simulations demonstrated that collaborative efforts among multiple aircraft could substantially reduce the required overload, particularly in scenarios involving rapid maneuvers, which are also known as “bang–bang” maneuvers. Building on this foundational work, Nikusokhan and Nobahari [12] introduced a cooperative guidance law designed to intercept targets with unpredictable maneuvers, using principles of optimal control theory. They framed the cooperative guidance challenge as an optimal control problem, where aircraft energy consumption was used as an optimization metric. By solving this problem, they identified optimal parameters for the guidance law and established its superiority over proportional guidance through numerical simulations. Zhao *et al.* [13] built on the concept of proportional guidance to propose a cooperative guidance strategy tailored for multiple aircraft salvo attacks. This strategy integrated a proportional guidance component for target engagement with a cooperative coordination guidance component to ensure simultaneous impacts on the maneuvering targets. Then, expanding on this approach, Zhao and Zhou [14] extended their method to three-dimensional space and demonstrated through theoretical analysis and numerical simulations its applicability to cooperative attacks on both stationary and maneuvering targets. Under switching topology conditions, Zhao *et al.* [15] transformed the challenge of cooperative attacks on maneuvering targets into a time-varying formation tracking problem. This transformation provided a systematic approach to designing guidance law parameters and a mathematical proof of the guidance law’s convergence. Wang and Tan [16] proposed a comprehensive three-dimensional cooperative guidance law for engaging maneuvering targets when multiple aircraft were assigned specific impact angles. This guidance law incorporated individual and cooperative components. The individual component enabled each aircraft to independently approach the desired impact angle and facilitated impacts from multiple directions. The cooperative component utilized the neighboring information to ensure that all aircraft simultaneously impacted the target. The introduction of robust control principles by Liu *et al.* [17] improved the cooperative guidance design, so the resulting method enabled simultaneous target impacts while effectively mitigating the input saturation. Zhai *et al.* [18] introduced a time-varying terminal sliding mode guidance law, which addressed the challenge of simultaneously intercepting maneuvering targets. Their method achieved simultaneous impacts even under uncertain target acceleration conditions and mitigated the singularity and chattering issues associated with sliding mode control due to enhancements in the sliding mode surface design. Wang *et al.* [19] developed a cooperative guidance law with the LOS angle constraints variable for maneuvering targets. This method ensured simultaneous target impacts by utilizing the remaining distance as a coordination measure. Yu *et al.* [20, 21] examined the adaptive cooperation in time-varying formation tracking guidance for multiple aircraft. They developed an adaptive cooperative guidance law that enabled the lead aircraft to satisfy the impact angle constraints, while maintaining time-varying formation tracking among the participating aircraft. You *et al*. [22] designed a cooperative guidance law for controlled thrust missiles to intercept maneuvering targets. Their approach was based on the nonsingular terminal sliding mode control method, which ensured accurate impacts on maneuvering targets while adhering to the hit angle constraints.

While previous cooperative guidance methods achieved asymptotic convergence, the short duration of the end-guidance phase in maneuvering target scenarios required higher standards of convergence. Therefore, further research has addressed the design of finite-time convergent cooperative guidance laws for maneuvering targets. Song *et al.* [23] specifically addressed the terminal-stage cooperative guidance problem of multiple aircraft intercepting maneuvering targets. They proposed a cooperative guidance law that satisfied the impact angle constraints using the nonsingular terminal sliding mode control method. This law provided acceleration commands in the LOS tangent and normal directions, and was analyzed for finite-time stability using Lyapunov theory. Simulations confirmed its effectiveness. Jing *et al.* [24] focused on cooperative guidance under LOS angle constraints for maneuvering targets. They introduced a fixed-time convergent disturbance observer to estimate and compensate for disturbances caused by target maneuvering. Using this foundation, they developed a cooperative guidance law based on a fixed-time convergent consistency protocol to ensure the convergence of the LOS angle, LOS angular velocity, and impact time deviation of the aircraft. Liu *et al.* [25] explored the interception of hypersonic vehicles and designed an LOS direction guidance directive based on algebraic graph theory and consensus theory. They also created an LOS normal cooperative guidance law using a finite-time disturbance observer and sliding mode control methods. Numerical simulations confirmed the effectiveness of their designed cooperative guidance law. Chen *et al.* [26] examined the three-dimensional cooperative guidance problem for maneuvering targets. They proposed a fixed-time adaptive distributed guidance law in the LOS direction and perpendicular to it. This law was built on the concept of a fast nonsingular terminal sliding surface and ensured compliance with both impact time and angle constraints. Zhang and Zhang [27] designed a three-dimensional fixed-time convergence cooperative guidance law based on the fixed-time convergence theory for the problem of multiple missiles that simultaneously intercept maneuvering targets. This guidance law can simultaneously ensure the fixed-time convergence of the LOS angular rate and consistency of the impact time. Dong *et al.* [28] designed a fixed-time convergence cooperative guidance law for maneuvering targets, which achieved simultaneous impact on the targets while satisfying the constraints on the impact angle. Based on the integral sliding mode theory and fixed-time convergence theory, the cooperative guidance law was designed in the LOS direction and the LOS normal direction, the fixed-time convergence stability of the guidance law was theoretically proven, and the convergence time was estimated.

Recent studies on cooperative guidance, such as [29]'s decentralized approach with maneuverability awareness and [30]'s fixed-time nonsingular terminal sliding mode method, have advanced target interceptions under specific constraints. However, [29] relies on complex acceleration estimation and lacks input saturation handling, while [30] risks excessive initial commands and limited topological adaptability. In contrast, the proposed finite-time cooperative guidance (FnTCG) law offers broader applicability to both stationary and maneuvering targets, supports directed communication topologies, and employs a finite-time ESO for efficient disturbance estimation. By integrating saturation functions, FnTCG law avoids chattering and singularities, ensuring rapid convergence of time-to-go and terminal LOS angles, making it a more robust and practical solution for complex cooperative engagements.

Although the above works have made great efforts in cooperative guidance law design, there remain some limitations, such as directed topology, singularity, and overload constraint. Therefore, the cooperative guidance law is worthy of further investigation. Inspired by the above investigation, this paper proposes a FnTCG law for multiple aircraft to achieve a salvo attack with different terminal angles. In contrast to the literature, this paper's main contributions are as follows:

(1) Compared to cooperative guidance laws presented in [5–9], the proposed FnTCG law is effective for both fixed and maneuvering targets. Specifically, it addresses maneuvering targets with unknown acceleration, presenting a more complex challenge than that posed by stationary targets.
(2) In contrast to existing cooperative guidance laws that exhibit asymptotic stability [10–22], the proposed FnTCG law is designed to synchronize impact times and achieve the desired terminal angles within a finite time frame. Given that terminal guidance for maneuvering targets must be executed swiftly, the proposed FnTCG law aligns more closely with practical requirements.
(3) The guidance laws discussed in [23–28] have developed FnTCG laws for maneuvering targets; however, these methods are limited to undirected topologies. In comparison, the FnTCG law is applicable to directed topologies, offering a more generalized approach.
(4) Moreover, the methods outlined in [23, 24] necessitate that multiple aircraft achieve consensus on their velocities, which is not required for multi-aircraft operations and may lead to unnecessary energy expenditure. Additionally, approaches in [25–28] introduce linearization terms due to feedback linearization techniques, resulting in excessively large guidance commands during the initial phase and singularity issues at the terminal stage. In contrast, the proposed FnTCG law does not require velocity consensus among multiple aircraft. By directly addressing the control challenges of nonlinear systems, it effectively avoids the singularity problems associated with feedback linearization. Furthermore, the integration of saturation functions within the guidance law ensures adherence to acceleration constraints.

The remainder of this paper is organized as follows: The problem statement and preliminaries are provided in Sec. 2. The 3D cooperative guidance law considering the overload constraint is designed in Sec. 3. Section 4 presents the simulation results to verify the effectiveness of the proposed guidance law. Finally, Sec. 5 provides conclusion remarks.

2. Problem Statement and Preliminaries

2.1. *Problem statement*

The 3D guidance scenario in which N aircraft attack a maneuvering target is investigated. Figure 1 illustrates the 3D cooperative guidance geometry, where T is the target; $m_i, i \in \{1, 2, \ldots, N\}$ denotes the ith aircraft; $X_gY_gZ_g$ and $X_sY_sZ_s$ are the inertial frame and LOS frame, respectively; R_i is the LOS range; $q_{\varepsilon i}$ and $q_{\beta i}$ are the elevation LOS angle and azimuth LOS angle, respectively. The aircraft acceleration vector in the LOS frame is denoted by $\boldsymbol{a}_{Mi} = [a_{Mri}\ a_{M\varepsilon i}\ a_{M\beta i}]^{\mathrm{T}}$. For the target, $\boldsymbol{a}_{Ti} = [a_{Tri}\ a_{T\varepsilon i}\ a_{T\beta i}]^{\mathrm{T}}$ has similar notations to the ith aircraft.

The relative kinematic equations between the ith aircraft and the maneuvering target can be described by [23]

$$\begin{cases} \ddot{R}_i - R_i\dot{q}_{\varepsilon i}^2 - R_i\dot{q}_{\beta i}^2\cos^2 q_{\varepsilon i} = a_{Tri} - a_{Mri}, \\ R_i\ddot{q}_{\varepsilon i} + 2\dot{R}_i\dot{q}_{\varepsilon i} + R_i\dot{q}_{\beta i}^2\sin q_{\varepsilon i}\cos q_{\varepsilon i} = a_{T\varepsilon i} - a_{M\varepsilon i}, \\ -R_i\ddot{q}_{\beta i}\cos q_{\varepsilon i} - 2\dot{R}_i\dot{q}_{\beta i}\cos q_{\varepsilon i} + 2R_i\dot{q}_{\varepsilon i}\dot{q}_{\beta i}\sin q_{\varepsilon i} \\ \qquad = a_{T\beta i} - a_{M\beta i}. \end{cases} \tag{1}$$

Let the state variables be defined as $x_{1i} = R_i$, $x_{2i} = \dot{R}_i$, $x_{3i} = q_{\varepsilon i} - q_{\varepsilon di}$, $x_{4i} = \dot{q}_{\varepsilon i}$, $x_{5i} = q_{\beta i} - q_{\beta di}$ and $x_{6i} = \dot{q}_{\beta i}$, where $q_{\varepsilon di}$ and $q_{\beta di}$ are the desired impact angle sequences. Due to the difficulty in directly measuring the target's acceleration, $d_{\varepsilon i} = a_{T\varepsilon i}/R_i$ and $d_{\beta i} = -a_{T\beta i}/R_i\cos q_{\varepsilon i}$ are represented as disturbances. Therefore, (1) can be reformulated as follows:

$$\begin{cases} \dot{x}_{1i} = x_{2i}, \\ \dot{x}_{2i} = x_{1i}x_{4i}^2 + x_{1i}x_{6i}^2\cos^2 q_{\varepsilon i} - a_{Mri} + a_{Tri}, \\ \dot{x}_{3i} = x_{4i}, \\ \dot{x}_{4i} = -\dfrac{2x_{2i}}{x_{1i}}x_{4i} - x_{6i}^2\sin q_{\varepsilon i}\cos q_{\varepsilon i} - \dfrac{1}{x_{1i}}a_{M\varepsilon i} + d_{\varepsilon i}, \\ \dot{x}_{5i} = x_{6i}, \\ \dot{x}_{6i} = -\dfrac{2x_{2i}}{x_{1i}}x_{6i} + 2x_{4i}x_{6i}\tan q_{\varepsilon i} + \dfrac{1}{x_{1i}\cos q_{\varepsilon i}}a_{M\beta i} + d_{\beta i}. \end{cases} \tag{2}$$

A new variable $t_{go,i}$ is introduced to represent the remaining flight time of the aircraft, which can be approximately expressed as

$$t_{go,i} = -\frac{R_i}{\dot{R}_i}. \tag{3}$$

Taking the time derivative of (3) and combining it with (2) yield the following:

$$\dot{t}_{go,i} = -1 + \frac{x_{1i}^2}{x_{2i}^2}x_{4i}^2 + \frac{x_{1i}^2}{x_{2i}^2}x_{6i}^2\cos^2 q_{\varepsilon i} - \frac{x_{1i}}{x_{2i}^2}a_{Mri} + d_{ri}, \tag{4}$$

where $d_{ri} = x_{1i}a_{Tri}/x_{2i}^2$. Here, the unknown disturbances $d_{ri}, d_{\varepsilon i}, d_{\beta i}$ caused by the target maneuvers are assumed to satisfy certain conditions.

Assumption 1. The unknown disturbances $d_{ri}, d_{\varepsilon i}, d_{\beta i}$ caused by the target maneuvers satisfy the following condition:

$$\begin{cases} |d_{ri}| \le W, |d_{\varepsilon i}| \le W, |d_{\beta i}| \le W, \\ |\dot{d}_{ri}| \le \bar{W}, |\dot{d}_{\varepsilon i}| \le \bar{W}, |\dot{d}_{\beta i}| \le \bar{W}, \end{cases}$$

where W and $\bar{W}$ are positive constants.

Based on (2) and (4), the cooperative guidance law can be divided into two parts. The first part designs the guidance law in the LOS normal direction, which ensures that the LOS angular rates of multiple aircraft converge to the origin, and the LOS angles converge to the desired sequence. The second part designs the guidance law in the LOS direction to synchronize the remaining flight time of multiple aircraft. According to the above analysis, Definition 1 provides the specific form of the cooperative guidance law to achieve a finite-time cooperative attack.

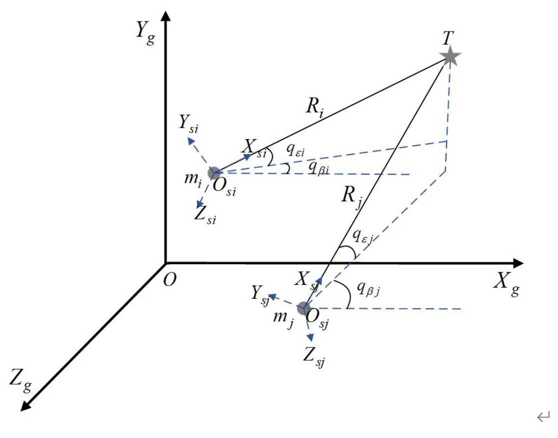

Fig. 1. Three-dimensional cooperative guidance geometry.

Definition 1. For any aircraft $m_1, m_2, \dots, m_N$, considering

$$\begin{cases} \lim\limits_{t\to\bar{t}}(x_{3i}(t) - x_{3j}(t)) = 0, \\ \lim\limits_{t\to\bar{t}} x_{4i}(t) = 0, \\ \lim\limits_{t\to\bar{t}}(x_{5i}(t) - x_{5j}(t)) = 0 \quad \forall\, i,j \in \{1,2,\dots,N\}, \\ \lim\limits_{t\to\bar{t}} x_{6i}(t) = 0, \\ \lim\limits_{t\to\bar{t}}(t_{go,i}(t) - t_{go,j}(t)) = 0. \end{cases} \tag{5}$$

If (5) holds, multiple aircraft can impact the maneuvering targets simultaneously under desired LOS angle constraints. Here, $\bar{t}$ is the upper bound limit of the convergence time of the guidance law.

2.2. *Communication topology*

A directed graph $G = (\mathcal{V}, \mathcal{E})$ is developed for N agents to represent the interactions among the agents, vertex set and edge set. The edges are an ordered pair of vertices $\mathcal{V}$, which implies that agent j can receive information from agent i. If there is a directed edge from i to j, then i is defined as the parent node, j is defined as the child node, the neighbors of node i are represented by $\mathcal{N}_i = \{j \in \mathcal{V} \mid (v_j, v_i) \in \mathcal{E}\}$, and $|\mathcal{N}_i|$ are the neighbor numbers of agent i.

The adjacency matrix $\boldsymbol{A}$ associated with G is defined such that $a_{ij} = 1$ if $i \neq j$ and node i is neighboring to node j, and $a_{ij} = 0$ otherwise. For a directed graph G, matrix A is asymmetric. The Laplacian matrix of the graph associated with adjacency matrix $\boldsymbol{A}$ is $\boldsymbol{L} = (l_{ij})$, where $l_{ii} = \sum_{j=1}^{N} a_{ij}$ and $l_{ij} = -a_{ij}, i \neq j$. Assumption 2 describes the communication topology of the multiple aircraft systems.

Assumption 2. The communication topology of the multiple aircraft systems is directed, strongly connected, and detailed balanced.

Lemma 1 (31). *Under Assumption* 2, *there exists a positive column vector* $\boldsymbol{\theta} = (\theta_1, \dots, \theta_N)^{\mathrm{T}}$ *such that* $\theta_i a_{ij} = \theta_j a_{ji}$ *for all* $i, j = 1 \dots, N$. *Denote* $\Theta = \mathrm{diag}(\theta_1, \dots, \theta_N)$. *Then, the matrix* $\Theta\boldsymbol{L}$ *is symmetric.*

Lemma 2 (31). *Let* $\boldsymbol{L} \in \mathbb{R}^{N\times N}$ *be the Laplacian matrix of a directed graph G. If G is strongly connected, then* 0 *is a simple eigenvalue of* $\boldsymbol{L}$, *and* $\boldsymbol{1}_N$ *is the associated eigenvector*; *i.e.* $\boldsymbol{L}\boldsymbol{1}_N = 0$ *and all other* $N-1$ *eigenvalues have positive real parts.*

2.3. *Useful lemmas*

Definition 2. Consider the system $\dot{\xi} = f(\xi), f(0) = 0$, where $\xi \in \mathbb{R}^N$, $f(\xi) = (f_1(\xi), \dots, f_N(\xi))^{\mathrm{T}}$ is a continuous vector field. Let $(r_1, \dots, r_N) \in \mathbb{R}^N$ with $r_i > 0, i = 1, 2, \dots, N$. $f(\xi)$ is said to be homogeneous of degree $\kappa \in \mathbb{R}$ with respect to $(r_1, \dots, r_N)$, if for any given $\varepsilon > 0$, $f_i(\varepsilon^{r_1}\xi_1, \dots, \varepsilon^{r_N}\xi_N) = \varepsilon^{\kappa + r_i} f_i(\xi), i = 1, 2, \dots, N, \forall\, \xi \in \mathbb{R}^N$. System $\dot{\xi} = f(\xi), f(0) = 0$ is said to be homogeneous if $f(\xi)$ is homogeneous.

Lemma 3 (32). *Consider the following system*:

$$\dot{\xi} = f(\xi) + \hat{f}(\xi), \quad f(0) = 0, \quad \xi \in \mathbb{R}^N, \tag{6}$$

where $f(\xi)$ *is a continuous homogeneous vector field of degree* $\kappa < 0$ *with respect to* $(r_1, \dots, r_N)$, *and* $\hat{f}(\xi)$ *satisfies* $\hat{f}(0) = 0$. *Assume that* $\xi = 0$ *is an asymptotically stable equilibrium of the system* $\dot{\xi} = f(\xi)$. *Then,* $\xi = 0$ *is a locally finite-time stable equilibrium of the system if*

$$\lim_{\varepsilon\to 0} \frac{\hat{f}_i(\varepsilon^{r_1}\xi_1, \dots, \varepsilon^{r_N}\xi_N)}{\varepsilon^{k + r_i}} = 0, \quad i = 1, \dots, N, \quad \forall\, \xi \neq 0.$$

Moreover, if the stable equilibrium $\xi = 0$ *of the original system* (6) *is globally asymptotically stable, then* $\xi = 0$ *is a globally finite-time stable equilibrium of system* (6).

Lemma 4 (33). *Consider the following observation error system*:

$$\begin{cases} \dot{\sigma}_0 = -\lambda_0 L^{1/(n+1)} |\sigma_0|^{n/(n+1)} \operatorname{sign}(\sigma_0) + \sigma_1, \\ \dot{\sigma}_1 = -\lambda_1 L^{1/n} |\sigma_1 - \sigma_0|^{(n-1)/n} \operatorname{sign}(\sigma_1 - \sigma_0) + \sigma_2, \\ \vdots \\ \dot{\sigma}_{n-1} = -\lambda_{n-1} L^{1/2} |\sigma_{n-1} - \sigma_{n-2}|^{(1)/2} \\ \quad \times \operatorname{sign}(\sigma_{n-1} - \sigma_{n-2}), + \sigma_n \\ \dot{\sigma}_n = -\lambda_n L \operatorname{sign}(\sigma_n - \sigma_{n-1}) + [-L, L], \end{cases} \tag{7}$$

where $L > 0$, *and* $\lambda_i > 1, i = 0, 1, \dots, n$ *are suitable parameters. System* (7) *is convergent in finite time.*

3. 3D Cooperative Guidance Law Design

This section proposes a distributed cooperative guidance law based on finite-time convergence theory and theoretically demonstrates that the designed distributed cooperative guidance law can achieve multi-directional simultaneous attack on maneuvering targets in finite time.

3.1. *Design of the finite-time extended state observer*

From (2) and (4), the guidance model contains disturbances $d_{ri}, d_{\varepsilon i}, d_{\beta i}$ caused by the unknown maneuver of the target. Since directly measuring the values of these disturbance terms is challenging, an observer must be designed to effectively estimate them.

Let $\hat{t}_{go,i}, \hat{d}_{ri}, \hat{x}_{3i}, \hat{x}_{4i}, \hat{d}_{\varepsilon i}, \hat{x}_{5i}, \hat{x}_{6i}, \hat{d}_{\beta i}$ be the estimated values of $t_{go,i}, d_{ri}, x_{3i}, x_{4i}, d_{\varepsilon i}, x_{5i}, x_{6i}, d_{\beta i}$, respectively, and let $\lambda_1, \lambda_2, \lambda_3, \lambda_4, \lambda_5, L$ be the observer parameters. Design the following finite-time extended state observer [34]:

$$\begin{cases} \dot{\hat{t}}_{go,i} = \varsigma_{1i} - 1 + \dfrac{x_{1i}^2}{x_{2i}^2} x_{4i}^2 + \dfrac{x_{1i}^2}{x_{2i}^2} x_{6i}^2 \cos^2 q_{\varepsilon i} - \dfrac{x_{1i}}{x_{2i}^2} a_{Mri}, \\ \varsigma_{1i} = -\lambda_1 L^{\frac{1}{2}} \operatorname{sig}^{\frac{1}{2}}(\hat{t}_{go,i} - t_{go,i}) + \hat{d}_{ri}, \quad \dot{\hat{d}}_{ri} = \varsigma_{2i}, \\ \varsigma_{2i} = -\lambda_2 L \operatorname{sig}^{\frac{1}{2}}(\hat{d}_{ri} - \varsigma_{1i}), \quad \dot{\hat{x}}_{3i} = \varsigma_{3i}, \\ \varsigma_{3i} = -\lambda_3 L^{\frac{1}{3}} \operatorname{sig}^{\frac{2}{3}}(\hat{x}_{3i} - x_{3i}) + \hat{x}_{4i}, \\ \dot{\hat{x}}_{4i} = \varsigma_{4i} - \dfrac{2x_{2i}}{x_{1i}} x_{4i} - x_{6i}^2 \sin q_{\varepsilon i} \cos q_{\varepsilon i} - \dfrac{1}{x_{1i}} a_{M\varepsilon i}, \\ \varsigma_{4i} = -\lambda_4 L^{\frac{1}{2}} \operatorname{sig}^{\frac{1}{2}}(\hat{x}_{4i} - \varsigma_{3i}) + \hat{d}_{\varepsilon i}, \\ \dot{\hat{d}}_{\varepsilon i} = -\lambda_5 L \operatorname{sig}^{\frac{1}{2}}(\hat{d}_{\varepsilon i} - \varsigma_{4i}), \quad \dot{\hat{x}}_{5i} = \varsigma_{5i}, \\ \varsigma_{5i} = -\lambda_3 L^{\frac{1}{3}} \operatorname{sig}^{\frac{2}{3}}(\hat{x}_{5i} - x_{5i}) + \hat{x}_{6i}, \\ \dot{\hat{x}}_{6i} = \varsigma_{6i} - \dfrac{2x_{2i}}{x_{1i}} x_{6i} + 2x_{4i} x_{6i} \tan q_{\varepsilon i} + \dfrac{1}{x_{1i} \cos q_{\varepsilon i}} a_{M\beta i}, \\ \varsigma_{6i} = -\lambda_4 L^{\frac{1}{2}} \operatorname{sig}^{\frac{1}{2}}(\hat{x}_{6i} - \varsigma_{5i}) + \hat{d}_{\beta i}, \\ \dot{\hat{d}}_{\beta i} = -\lambda_5 L \operatorname{sig}^{\frac{1}{2}}(\hat{d}_{\beta i} - \varsigma_{6i}). \end{cases} \tag{8}$$

Define the estimation errors to be

$$\begin{aligned} &\tilde{t}_{go,i} = \hat{t}_{go,i} - t_{go,i}, \quad \tilde{d}_{ri} = \hat{d}_{ri} - d_{ri}, \\ &\tilde{x}_{3i} = \hat{x}_{3i} - x_{3i}, \quad \tilde{x}_{4i} = \hat{x}_{4i} - x_{4i}, \\ &\tilde{d}_{\varepsilon i} = \hat{d}_{\varepsilon i} - d_{\varepsilon i}, \quad \tilde{x}_{5i} = \hat{x}_{5i} - x_{5i}, \\ &\tilde{x}_{6i} = \hat{x}_{6i} - x_{6i}, \quad \tilde{d}_{\beta i} = \hat{d}_{\beta i} - d_{\beta i}. \end{aligned} \tag{9}$$

Then, from (2), (4) and (8), the following estimation error equation can be derived:

$$\begin{cases} \dot{\tilde{t}}_{go,i} = -\lambda_1 L^{\frac{1}{2}} \operatorname{sig}^{\frac{1}{2}}(\tilde{t}_{go,i}) + \tilde{d}_{ri}, \\ \dot{\tilde{d}}_{ri} = -\lambda_2 L \operatorname{sig}^{\frac{1}{2}}(\tilde{d}_{ri} - \dot{\tilde{t}}_{go,i}) - \dot{d}_{ri}, \\ \dot{\tilde{x}}_{3i} = -\lambda_3 L^{\frac{1}{3}} \operatorname{sig}^{\frac{2}{3}}(\tilde{x}_{3i}) + \tilde{x}_{4i}, \\ \dot{\tilde{x}}_{4i} = -\lambda_4 L^{\frac{1}{2}} \operatorname{sig}^{\frac{1}{2}}(\tilde{x}_{4i} - \dot{\tilde{x}}_{3i}) + \tilde{d}_{\varepsilon i}, \\ \dot{\tilde{d}}_{\varepsilon i} = -\lambda_5 L \operatorname{sig}^{\frac{1}{2}}(\tilde{d}_{\varepsilon i} - \dot{\tilde{x}}_{4i}) - \dot{d}_{\varepsilon i}, \\ \dot{\tilde{x}}_{5i} = -\lambda_3 L^{\frac{1}{3}} \operatorname{sig}^{\frac{2}{3}}(\tilde{x}_{5i}) + \tilde{x}_{6i}, \\ \dot{\tilde{x}}_{6i} = -\lambda_4 L^{\frac{1}{2}} \operatorname{sig}^{\frac{1}{2}}(\tilde{x}_{6i} - \dot{\tilde{x}}_{5i}) + \tilde{d}_{\beta i}, \\ \dot{\tilde{d}}_{\beta i} = -\lambda_5 L \operatorname{sig}^{\frac{1}{2}}(\tilde{d}_{\beta i} - \dot{\tilde{x}}_{6i}) - \dot{d}_{\beta i}. \end{cases} \tag{10}$$

Based on Assumption 1, we obtain $|\dot{d}_{ri}| \le \bar{W}, |\dot{d}_{\varepsilon i}| \le \bar{W}, |\dot{d}_{\beta i}| \le \bar{W}$, where $\bar{W}$ is a positive constant. Therefore, according to Lemma 4, if the observer parameters satisfy

$$\lambda_1 > 1, \quad \lambda_2 > 1, \quad \lambda_3 > 1, \quad \lambda_4 > 1, \quad \lambda_5 > 1, \quad L > \bar{W} \tag{11}$$

the observation error (10) converges in finite time, i.e.

$$\begin{aligned} &\hat{t}_{go,i}(t) \equiv t_{go,i}(t), \quad \hat{d}_{ri}(t) \equiv d_{ri}(t), \\ &\hat{x}_{3i}(t) \equiv x_{3i}(t), \quad \hat{x}_{4i}(t) \equiv x_{4i}(t), \\ &\hat{d}_{\varepsilon i}(t) \equiv d_{\varepsilon i}(t), \quad \hat{x}_{5i}(t) \equiv x_{5i}(t), \\ &\hat{x}_{6i}(t) \equiv x_{6i}(t), \quad \hat{d}_{\beta i}(t) \equiv d_{\beta i}(t), \end{aligned} \quad \forall\, t > T_1. \tag{12}$$

3.2. *Normal acceleration design*

In this section, the normal acceleration commands are derived. These guidance laws ensure that the elevation and azimuth LOS angles and their corresponding angular rates rapidly converge in finite time, so that multiple aircraft can hit the maneuvering target at the desired terminal LOS angles.

From the relative kinematic equation (2), the guidance equation in the elevation LOS angle direction is obtained as

$$\begin{cases} \dot{x}_{3i} = x_{4i}, \\ \dot{x}_{4i} = -\dfrac{2x_{2i}}{x_{1i}} x_{4i} - x_{6i}^2 \sin q_{\varepsilon i} \cos q_{\varepsilon i} - \dfrac{1}{x_{1i}} a_{M\varepsilon i} + d_{\varepsilon i.} \end{cases} \tag{13}$$

The guidance equation in the azimuth LOS angle direction is obtained as

$$\begin{cases} \dot{x}_{5i} = x_{6i}, \\ \dot{x}_{6i} = -\dfrac{2x_{2i}}{x_{1i}} x_{6i} + 2x_{4i} x_{6i} \tan q_{\varepsilon i} + \dfrac{1}{x_{1i} \cos q_{\varepsilon i}} a_{M\beta i} + d_{\beta i}. \end{cases} \tag{14}$$

First, consider the guidance model (13) in the elevation LOS angle direction. Design the following cooperative guidance law:

$$a_{M\varepsilon i} = a_{M\varepsilon i}^a + a_{M\varepsilon i}^b, \tag{15}$$

where

$$\begin{cases} a_{M\varepsilon i}^a = x_{1i}\left(-\dfrac{2x_{2i}}{x_{1i}} x_{4i} - x_{6i}^2 \sin q_{\varepsilon i} \cos q_{\varepsilon i} + \hat{d}_{\varepsilon i}\right), \\ a_{M\varepsilon i}^b = k_1 \displaystyle\sum_{j=1}^{N} a_{ij} \operatorname{sig}^{\alpha_1}(x_{3i} - x_{3j}) + k_2 \operatorname{sig}^{\alpha_2}(x_{4i}). \end{cases} \tag{16}$$

Theorem 1. *Under assumptions* 1 *and* 2, *if the guidance parameters satisfy* $k_1 > 0$, $k_2 > 0$, $0 < \alpha_1 < 1$, $\alpha_2 = 2\alpha_1/(1+\alpha_1)$, *then the designed cooperative guidance law* (15) *can ensure that multiple aircraft achieve the terminal elevation LOS angle cooperation in a finite time.*

Proof. Substituting (15) into (13), we obtain

$$\begin{cases} \dot{x}_{3i} = x_{4i}, \\ \dot{x}_{4i} = -\dfrac{1}{x_{1i}}\left(k_1 \operatorname{sig}^{\alpha_1}\left(\displaystyle\sum_{j=1}^{N} a_{ij}(x_{3i} - x_{3j})\right)\right. \\ \qquad\left. + k_2 \operatorname{sig}^{\alpha_2}(x_{4i})\right) + \tilde{d}_{\varepsilon i}. \end{cases} \tag{17}$$

Let

$$\begin{cases} \boldsymbol{\xi}_3 = \boldsymbol{M}\boldsymbol{x}_3, \\ \boldsymbol{\xi}_4 = \boldsymbol{x}_4, \end{cases} \tag{18}$$

where $\boldsymbol{x}_3 = [x_{31}, x_{32}, \dots, x_{3N}]^{\mathrm{T}}$, $\boldsymbol{x}_4 = [x_{41}, x_{42}, \dots, x_{4N}]^{\mathrm{T}}$. $\boldsymbol{M} = \boldsymbol{I} - \boldsymbol{1}_N\boldsymbol{\chi}^{\mathrm{T}}$ and $\boldsymbol{\chi} = [\chi_1, \chi_2, \dots, \chi_N]^{\mathrm{T}}$ satisfy $\boldsymbol{\chi}^{\mathrm{T}}\boldsymbol{L} = 0$ and $\boldsymbol{\chi}^{\mathrm{T}}\boldsymbol{1} = 1$. According to the algebraic properties of matrix $\boldsymbol{M}$, if and only if $x_{31} = x_{32} = \cdots = x_{3N}$ and $x_{41} = x_{42} = \cdots = x_{4N} = 0$, we can obtain $\boldsymbol{\xi}_3 = \boldsymbol{0}$ and $\boldsymbol{\xi}_4 = \boldsymbol{0}$. According to (16) and (17), the derivatives of $\boldsymbol{\xi}_3$ and $\boldsymbol{\xi}_4$ satisfy:

$$\begin{cases} \dot{\boldsymbol{\xi}}_3 = \boldsymbol{M}\boldsymbol{\xi}_4, \\ \dot{\boldsymbol{\xi}}_4 = -\boldsymbol{\gamma}(k_1 \operatorname{sig}^{\alpha_1}(\boldsymbol{L}\boldsymbol{\xi}_3) + k_2 \operatorname{sig}^{\alpha_2}(\boldsymbol{\xi}_4)) + \tilde{\boldsymbol{d}}_\varepsilon, \end{cases} \tag{19}$$

where $\boldsymbol{\gamma} = \operatorname{diag}\{1/x_{11}, 1/x_{12}, \dots, 1/x_{1N}\}$, $\tilde{\boldsymbol{d}}_\varepsilon = [\tilde{d}_{\varepsilon 1}, \tilde{d}_{\varepsilon 2}, \dots, \tilde{d}_{\varepsilon N}]^{\mathrm{T}}$.

According to Lemma 1, under Assumption 2, there exists a positive definite matrix $\boldsymbol{\varsigma} = \operatorname{diag}\{\varsigma_1, \varsigma_2, \dots, \varsigma_N\}$ such that $\boldsymbol{\varsigma}\boldsymbol{L} = (\boldsymbol{\varsigma}\boldsymbol{L})^{\mathrm{T}}$. We select the following Lyapunov function:

$$V_1 = k_1 \int_0^{\boldsymbol{L}\xi_3} \boldsymbol{\varsigma}\boldsymbol{\gamma}\operatorname{sig}^{\alpha_1}(s)\mathrm{d}s + \frac{1}{2}\boldsymbol{\xi}_4^{\mathrm{T}}(\boldsymbol{\varsigma}\boldsymbol{L})\boldsymbol{\xi}_4. \tag{20}$$

First, the selected Lyapunov function must be proven to be positive definite. Since $\boldsymbol{L}\boldsymbol{\xi}_3$ and $\operatorname{sig}^{\alpha_1}(\boldsymbol{L}\boldsymbol{\xi}_3)$ have identical signs, and according to the definition of $\boldsymbol{\gamma}$, it is known to be positive definite. Therefore, $\int_0^{\boldsymbol{L}\xi_3} \boldsymbol{\varsigma}\boldsymbol{\gamma}\operatorname{sig}^{\alpha_1}(s)\mathrm{d}s \geq 0$. In addition, $\int_0^{\boldsymbol{L}\xi_3} \boldsymbol{\varsigma}\boldsymbol{\gamma}\operatorname{sig}^{\alpha_1}(s)\mathrm{d}s = 0$ if and only if $\boldsymbol{L}\boldsymbol{\xi}_3 = 0$. According to Lemma 1, when $\boldsymbol{L}\boldsymbol{\xi}_3 = 0$, it can be derived that

$$\boldsymbol{\xi}_3 = k\boldsymbol{1}, \quad k \in \mathbb{R}. \tag{21}$$

Furthermore, based on the definitions of $\boldsymbol{M}$ and $\boldsymbol{\chi}$, we have

$$\boldsymbol{\chi}^{\mathrm{T}}\boldsymbol{M} = \boldsymbol{\chi}^{\mathrm{T}}\boldsymbol{I} - \boldsymbol{\chi}^{\mathrm{T}}\boldsymbol{1}\boldsymbol{\chi}^{\mathrm{T}} = \boldsymbol{0}. \tag{22}$$

By combining (18) and (22), we obtain

$$\boldsymbol{\chi}^{\mathrm{T}}\boldsymbol{\xi}_3 = \boldsymbol{\chi}^{\mathrm{T}}\boldsymbol{M}\boldsymbol{x}_3 = 0. \tag{23}$$

Substituting (21) into (23) yields $k = 0$. Hence, $\boldsymbol{L}\boldsymbol{\xi}_3 = 0$ and $\boldsymbol{\xi}_3 = 0$ are equivalent. Consequently, for any $\boldsymbol{\xi}_3 \neq \boldsymbol{0}$, it holds that $\int_0^{\boldsymbol{L}\xi_3} \operatorname{sig}^{\alpha_1}(s)\mathrm{d}s > 0$. Moreover, since $\boldsymbol{\varsigma}\boldsymbol{L} = (\boldsymbol{\varsigma}\boldsymbol{L})^{\mathrm{T}}$, according to [28], it can be inferred that

$$\boldsymbol{\xi}_4^{\mathrm{T}}(\boldsymbol{\varsigma}\boldsymbol{L})\boldsymbol{\xi}_4 \geq \lambda(\boldsymbol{\varsigma}\boldsymbol{L})\|\boldsymbol{\xi}_4\|^2 > 0. \tag{24}$$

Thus, the selected Lyapunov function V_1 is positive definite when $k_1 > 0$. The derivative of V_1 along (19) satisfies

$$\begin{aligned} \dot{V}_1 &= k_1(\boldsymbol{L}\dot{\boldsymbol{\xi}}_3)^{\mathrm{T}}\boldsymbol{\varsigma}\boldsymbol{\gamma}\operatorname{sig}^{\alpha_1}(\boldsymbol{L}\xi_3) + \boldsymbol{\xi}_4^{\mathrm{T}}\boldsymbol{\varsigma}\boldsymbol{L}\dot{\boldsymbol{\xi}}_4 \\ &= k_1\boldsymbol{\xi}_3^{\mathrm{T}}\boldsymbol{L}^{\mathrm{T}}\boldsymbol{\varsigma}\boldsymbol{\gamma}\operatorname{sig}^{\alpha_1}(\boldsymbol{L}\boldsymbol{\xi}_3) \\ &\quad - k_1\boldsymbol{\xi}_4^{\mathrm{T}}\boldsymbol{\varsigma}\boldsymbol{\gamma}\boldsymbol{L}\operatorname{sig}^{\alpha_1}(\boldsymbol{L}\boldsymbol{\xi}_4) \\ &\quad - k_2\boldsymbol{\xi}_4^{\mathrm{T}}\boldsymbol{\varsigma}\boldsymbol{\gamma}\boldsymbol{L}\operatorname{sig}^{\alpha_2}(\boldsymbol{\xi}_4) + \boldsymbol{\xi}_4^{\mathrm{T}}\boldsymbol{\varsigma}\boldsymbol{L}\tilde{\boldsymbol{d}}_\varepsilon \\ &= -k_2\boldsymbol{\xi}_4^{\mathrm{T}}\boldsymbol{\varsigma}\boldsymbol{\gamma}\boldsymbol{L}\operatorname{sig}^{\alpha_2}(\boldsymbol{\xi}_4) + \boldsymbol{\xi}_4^{\mathrm{T}}\boldsymbol{\varsigma}\boldsymbol{L}\tilde{\boldsymbol{d}}_\varepsilon. \end{aligned} \tag{25}$$

Notably, based on the definition of $\dot{q}_i$, $\boldsymbol{\xi}_4$ is bounded in $[0, T_1)$. Furthermore, since $\tilde{\boldsymbol{d}}_\varepsilon$ is bounded in $[0, T_1)$, $\boldsymbol{\xi}_4^{\mathrm{T}}\boldsymbol{L}\tilde{\boldsymbol{d}}_\varepsilon$ is also bounded in $[0, T_1)$. Assuming that the upper bound of $\boldsymbol{\xi}_4^{\mathrm{T}}\boldsymbol{\varsigma}\boldsymbol{L}\tilde{\boldsymbol{d}}_\varepsilon$ is $\bar{d}_\varepsilon$, it follows that

$$\dot{V}_1 \leq -k_2\boldsymbol{\xi}_4^{T}\boldsymbol{\varsigma}\boldsymbol{L}\operatorname{sig}^{\alpha_2}(\boldsymbol{\xi}_4) + \bar{d}_\varepsilon \leq \bar{d}_\varepsilon. \tag{26}$$

Therefore, V_1 is bounded in $[0, T_1)$. When $t \geq T_1$, $\tilde{\boldsymbol{d}}_\varepsilon = 0$, in which case

$$\dot{V}_1 \leq -k_2\boldsymbol{\xi}_4^{\mathrm{T}}\boldsymbol{\varsigma}\boldsymbol{\gamma}\boldsymbol{L}\operatorname{sig}^{\alpha_2}(\boldsymbol{\xi}_4) \leq 0. \tag{27}$$

If $\dot{V}_1 = 0$, according to 23, $\boldsymbol{\xi}_3 = \boldsymbol{\xi}_4 = 0$. According to the Invariance-Like Theorem [34], system 23 is asymptotically stable.

Next, it will be shown that the system 23 is homogeneous with a negative homogeneity degree. To demonstrate this, let $\boldsymbol{\zeta}_1 = [x_{31}, x_{32}, \dots, x_{3N}, x_{41}, x_{42}, \dots, x_{4N}]^{\mathrm{T}} \in \mathbb{R}^{2N}$, its derivative is $\dot{\boldsymbol{\zeta}}_1 = f(\boldsymbol{\zeta}_1)$, and we have

$$\begin{aligned} & f_i(\varepsilon^{\lambda_1}x_{31}, \dots, \varepsilon^{\lambda_N}x_{3N}, \varepsilon^{\lambda_{N+1}}x_{41}, \dots, \varepsilon^{\lambda_{2N}}x_{4N})^{\mathrm{T}} \\ &= \varepsilon^{\lambda_{N+1}}x_{4i} - \sum_{j=1}^{N}\chi_j\varepsilon^{\lambda_{N+1}}x_{4j} \\ &= \varepsilon^{\lambda_{N+1}}\left(x_{4i} - \sum_{j=1}^{N}\chi_j x_{4j}\right) \\ &= \varepsilon^{K+\lambda_1}f_i(x_{31}, \dots, x_{3N}, x_{41}, \dots, x_{4N})^{\mathrm{T}} \\ & f_{N+i}(\varepsilon^{\lambda_1}x_{31}, \dots, \varepsilon^{\lambda_N}x_{3N}, \varepsilon^{\lambda_{N-1}}x_{41}, \dots, \varepsilon^{\lambda_{2N}}x_{4N})^{\mathrm{T}} \\ &= -k_1\frac{1}{R_i}\operatorname{sig}\left(\sum_{i=1}^{N}a_{ij}(\varepsilon^{\lambda_1}\xi_{1i} - \varepsilon^{\lambda_j}\xi_{1j})\right)^{\alpha_1} \\ &\quad -k_2\frac{1}{R_i}\operatorname{sig}(\varepsilon^{\lambda_{N+1}}\xi_{2i})^{\alpha_2} \\ &= \varepsilon^{\kappa+\lambda_{N+1}}f_i(x_{31}, \dots, x_{3N}, x_{41}, \dots, x_{4N})^{\mathrm{T}}. \end{aligned}$$

Through the above equation, it can be derived that

$$\begin{cases}\lambda_{N+i} = \lambda_i + \kappa,\\ \lambda_i = \lambda_j,\\ \lambda_i\alpha_1 = \kappa + \lambda_{N+i},\\ \lambda_{N+i}\alpha_2 = \kappa + \lambda_{N+i}.\end{cases}$$

Let $\lambda_i = 2$ and $\alpha_2 = 2\alpha_1/(1+\alpha_1)$; then, the homogeneity degree of the system is $\kappa = \alpha_1 - 1$. Furthermore, since $0 < \alpha_1 < 1$, system (23) is homogeneous with a negative homogeneity degree. According to Lemma 2, the state of system (23) converges to the origin in finite time. Thus, the cooperative target of achieving the terminal elevation LOS angle, as defined in Definition 2, is feasible. This completes the proof. □

Next, let us consider guidance (13) and design the following guidance law for the azimuth LOS angle direction:

$$a_{M\beta i} = a^a_{M\beta i} + a^b_{M\beta i}, \tag{28}$$

where

$$\begin{aligned} a^a_{M\beta i} &= x_{1i}\cos q_{\varepsilon i} \\ &\quad\times\left(-\frac{2x_{2i}}{x_{1i}}\dot{q}_{\beta i} + 2\dot{q}_{\varepsilon i}\dot{q}_{\beta i}\tan q_{\varepsilon i} + \hat{d}_{\beta i}\right),\\ a^b_{M\beta i} &= \cos q_{\varepsilon i}\left(-k_3\sum_{j=1}^{N} a_{ij}\,\mathrm{sig}^{\alpha_3}(x_{5i}-x_{5j})\right.\\ &\quad\left.- k_4\sum_{j=1}^{N} a_{ij}\,\mathrm{sig}^{\alpha_4}(x_{6i})\right). \end{aligned} \tag{29}$$

Theorem 2. *Under Assumptions* 1 *and* 2, *if the guidance parameters satisfy* $k_3 > 0$, $k_4 > 0$, $0 < \alpha_3 < 1$ *and* $\alpha_4 = 2\alpha_3/(1+\alpha_3)$, *then the proposed cooperative guidance law* (28) *ensures that multiple aircraft can achieve the terminal azimuth LOS angle cooperation in finite time.*

Proof. By substituting (28) into (13), we obtain

$$\begin{aligned} \dot{x}_{5i} &= x_{6i},\\ \dot{x}_{6i} &= -\frac{1}{x_{1i}}\left(k_3\sum_{j=1}^{N} a_{ij}\,\mathrm{sig}(x_{5i}-x_{5j})^{\alpha_3}\right.\\ &\quad\left.+ k_4\,\mathrm{sig}(x_{6i})^{\alpha_4}\right) + \tilde{d}_{\beta i}. \end{aligned} \tag{30}$$

Equation (30) has the same form as (17). Therefore, using the same analytical approach, we can prove that when the parameters satisfy $k_3 > 0, k_4 > 0, 0 < \alpha_3 < 1$ and $\alpha_4 = 2\alpha_3/(1+\alpha_3)$, there exists a finite time after which we obtain

$$x_{51} = x_{52} = \cdots = x_{5N},$$
$$x_{61} = x_{62} = \cdots = x_{6N} = 0.$$

By combining Theorems 1 and 2, we can conclude that there exists a finite time T_2 such that

$$\begin{cases} x_{31} = x_{32} = \cdots = x_{3N},\\ x_{41} = x_{42} = \cdots = x_{4N} = 0,\\ x_{51} = x_{52} = \cdots = x_{5N},\\ x_{61} = x_{62} = \cdots = x_{6N} = 0, \end{cases} \quad \forall\, t > T_2. \tag{31}$$

This completes the proof. □

3.3. *Tangential acceleration design*

According to Definition 2, the time-constrained objective is defined as

$$\lim_{t\to\bar{t}}(t_{go,i}(t) - t_{go,j}(t)) = 0, \quad \forall\, i,j \in \{1,2,\ldots,N\}. \tag{32}$$

To achieve this objective, the following cooperation guidance law is designed:

$$\begin{aligned} u_{ri} &= \frac{x_{2i}^2}{x_{1i}}\hat{d}_{ri} + k_5\tanh\\ &\quad\times\left(\mathrm{sig}^{\alpha_5}\left(\sum_{j=1}^{N} a_{ij}\left(t_{go,i}-t_{go,j}\right)\right)\right), \end{aligned} \tag{33}$$

where the saturation function

$$\tanh(x) = (e^{x/3} - e^{-x/3})/(e^{x/3} + e^{-x/3})$$

is restricted to the range of $[-1, 1]$.

Theorem 3. *Under Assumptions* 1 *and 2, if the guidance parameters satisfy* $k_5 > 0, 0 < \alpha_5 < 1$, *then the designed cooperative guidance law* (33) *can guarantee the consensus of* $t_{go,i}$ *to achieve a salvo attack within a finite time.*

Proof. By substituting the cooperative guidance law (33) into (4), we can deduce that

$$\begin{aligned} \dot{t}_{go,i} &= -1 + \frac{x_{1i}^2}{x_{2i}^2}\dot{q}_{\varepsilon i}^2 + \frac{x_{1i}^2}{x_{2i}^2}\dot{q}_{\beta i}^2\cos^2 q_{\varepsilon i} - k_5\frac{x_{1i}}{x_{2i}^2}\\ &\quad\times\tanh\left(\mathrm{sig}^{\alpha_5}\left(\sum_{j=1}^{N} a_{ij}\left(t_{go,i}-t_{go,j}\right)\right)\right) - \tilde{d}_{ri}. \end{aligned} \tag{34}$$

By letting $\boldsymbol{x} = [t_{go,1}, t_{go,2}, \ldots, t_{go,N}]^{\mathrm{T}}$, (34) can be rewritten as

$$\dot{\boldsymbol{x}} = -\mathbf{1}_n + \boldsymbol{\Phi} - k_5\boldsymbol{r}\tanh(\mathrm{sig}^{\alpha_5}(\boldsymbol{Lx})) - \tilde{\boldsymbol{d}}_r, \tag{35}$$

where

$$\boldsymbol{\Phi} = \operatorname{diag}\left(\frac{x_{11}^2}{x_{21}^2}\dot{q}_{\varepsilon 1}^2 + \frac{x_{11}^2}{x_{21}^2}\dot{q}_{\beta 1}^2 \cos^2 q_{\varepsilon 1}, \frac{x_{12}^2}{x_{22}^2}\dot{q}_{\varepsilon 2}^2 + \frac{x_{12}^2}{x_{22}^2}\dot{q}_{\beta 2}^2 \cos^2 q_{\varepsilon 2}, \dots, \frac{x_{1N}^2}{x_{2N}^2}\dot{q}_{\varepsilon N}^2 + \frac{x_{1N}^2}{x_{2N}^2}\dot{q}_{\beta N}^2 \cos^2 q_{\varepsilon N}\right), \tag{36}$$

$$\tilde{\boldsymbol{d}}_r = (\tilde{d}_{r1}, \tilde{d}_{r2}, \dots, \tilde{d}_{rN})^{\mathrm{T}},$$

$$\boldsymbol{r} = \operatorname{diag}\left(\frac{x_{11}}{x_{21}^2}, \frac{x_{12}^2}{x_{22}^2}, \dots, \frac{x_{1N}}{x_{2N}^2}\right).$$

□

By letting $\boldsymbol{\zeta} = \boldsymbol{M}\boldsymbol{x}$, it follows from (35) that the derivative of $\boldsymbol{\zeta}$ satisfies:

$$\dot{\boldsymbol{\zeta}} = -k_5 \boldsymbol{M}\boldsymbol{r} \tanh(\operatorname{sig}^{\alpha_5}(\boldsymbol{L}\boldsymbol{\zeta})) + \boldsymbol{M}\boldsymbol{\Phi} - \boldsymbol{M}\tilde{\boldsymbol{d}}_r. \tag{37}$$

According to the algebraic properties of matrix $\boldsymbol{M}$, we obtain $\boldsymbol{\zeta} = 0$ if and only if $t_{go,1} = t_{go,2} = \cdots = t_{go,N}$. Therefore, the next step is to prove that (37) converges in a finite time. Near the origin, $\tanh(\operatorname{sig}^{\alpha}(x)) = \operatorname{sig}^{\alpha}(x) + o(\operatorname{sig}^{\alpha}(x))$. Thus, near the origin, system (37) can be rewritten as

$$\dot{\boldsymbol{\zeta}} = -k_5 \boldsymbol{M}\boldsymbol{r} \operatorname{sig}^{\alpha_5}(\boldsymbol{L}\zeta) + \boldsymbol{M}\boldsymbol{\Phi} - \boldsymbol{M}\tilde{\boldsymbol{d}}_r + f(\boldsymbol{\zeta}), \tag{38}$$

where $f(\boldsymbol{\zeta}) = -k_5 \boldsymbol{M}\boldsymbol{r} o(\operatorname{sig}^{\alpha_5}(\boldsymbol{L}\boldsymbol{\zeta}))$. According to Lemma 3, if the following conditions are satisfied, then the state of system (38) converges to zero in finite time:

(1) The original system (37) is globally asymptotically stable.
(2) The following system is globally asymptotically stable and is a homogeneous system:

$$\dot{\boldsymbol{\zeta}} = -k_5 \boldsymbol{M}\boldsymbol{r} \operatorname{sig}^{\alpha_5}(\boldsymbol{L}\boldsymbol{\zeta}) + \boldsymbol{M}\boldsymbol{\Phi} - \boldsymbol{M}\tilde{\boldsymbol{d}}_r. \tag{39}$$

(3) $f(\boldsymbol{\zeta})$ satisfies $\lim_{\varepsilon \to 0} f(\varepsilon^{\eta_1}\boldsymbol{\zeta})/\varepsilon^{\kappa + r_1} = 0$, where $\kappa < 0, r_1 > 0$.

First, it is proven that the original system (37) is globally asymptotically stable. For this purpose, the Lyapunov function is selected to be $V_2 = \boldsymbol{\zeta}^{\mathrm{T}} \boldsymbol{\varsigma} \boldsymbol{L} \boldsymbol{\zeta}/2$. Since $\boldsymbol{\varsigma}\boldsymbol{L} = (\boldsymbol{\varsigma}\boldsymbol{L})^{\mathrm{T}}$, we obtain

$$\boldsymbol{\zeta}^{\mathrm{T}} \boldsymbol{\varsigma} \boldsymbol{L} \boldsymbol{\zeta} \geq \lambda(\boldsymbol{\varsigma}\boldsymbol{L}) \|\zeta\|^2 > 0. \tag{40}$$

Hence, V_2 is positive definite, and its derivation along system (37) satisfies

$$\dot{V}_2 = -k_5 \boldsymbol{\zeta}^{\mathrm{T}} \boldsymbol{\varsigma} \boldsymbol{L} \boldsymbol{M} \boldsymbol{r} \tanh(\operatorname{sig}^{\alpha_5}(\boldsymbol{L}\boldsymbol{\zeta})) - \boldsymbol{\zeta}^{\mathrm{T}} \boldsymbol{\varsigma} \boldsymbol{L} \boldsymbol{M} \tilde{\boldsymbol{d}}_r + \boldsymbol{\zeta}^{\mathrm{T}} \boldsymbol{\varsigma} \boldsymbol{L} \boldsymbol{M} \boldsymbol{\Phi}. \tag{41}$$

Based on the definitions of $\boldsymbol{\zeta}$ and $\boldsymbol{\Phi}, V_2$ is bounded in $[0, T_2)$. According to Theorems 1 and 2, $\tilde{\boldsymbol{d}}_r = \boldsymbol{0}$ and $\boldsymbol{\Phi} = 0$ hold when $t \geq T_2$. Thus, (41) is rewritten as

$$\dot{V}_2 = -k_5 \boldsymbol{\zeta}^{\mathrm{T}} \boldsymbol{L}^{\mathrm{T}} \boldsymbol{\varsigma} \boldsymbol{M} \boldsymbol{r} \tanh(\operatorname{sig}^{\alpha_5}(\boldsymbol{L}\boldsymbol{\zeta})). \tag{42}$$

Since matrix $\boldsymbol{r}$ is positive definite, $\boldsymbol{L}\boldsymbol{\zeta}$ and $\tanh(\operatorname{sig}^{\alpha_5} \times (\boldsymbol{L}\boldsymbol{\zeta}))$ have the same sign, and it can be deduced that $\dot{V}_2 \leq 0$. Therefore, $\boldsymbol{\zeta} = 0$ can be inferred from $\dot{V}_2 = 0$. According to the Invariance-Like Theorem [34], system (37) is globally asymptotically stable. To prove that system (37) is stable in finite time, according to Lemma 3, it is required to demonstrate that system (37) is homogeneous with a negative homogeneity degree. Let $\dot{\boldsymbol{\zeta}} = f(\boldsymbol{\zeta})$ according to Definition 1, it follows that

$$f_i(\varepsilon^{\delta}\zeta_1, \varepsilon^{\delta}\zeta_2, \dots, \varepsilon^{\delta}\zeta_N) = \varepsilon^{\alpha_j \delta} f(\zeta_i) = \varepsilon^{\delta + \kappa} f(\zeta_i), \tag{43}$$

when $0 < \alpha_5 < 1$, system (37) becomes a homogeneous system with a negative homogeneity degree. Finally, using a similar method to that in [35], it can be easily proven that $\lim_{\varepsilon \to 0} f(\varepsilon^{r_1}\boldsymbol{\zeta})/\varepsilon^{\kappa + r_1} = 0$ when $\kappa < 0, r_1 > 0$. Therefore, according to Lemma 3, system (38) is globally stable in finite time, which indicates that the salvo attack target given by (32) can be achieved within a finite time.

Remark 1. From (15) and (28), it can be observed that no terms approaching zero appear in the denominator of the cooperative guidance law in the LOS normal direction. Additionally, the remaining components of the guidance law involve only simple algebraic operations on state variables, thereby effectively preventing singularities in the guidance commands. In contrast, conventional cooperative guidance laws typically require feedback linearization to transform the nonlinear guidance model into a linearized form. During this process, denominators containing terms approaching zero (e.g. R) may arise, leading to singular guidance commands. Similarly, in the LOS tangential guidance law (33), the first term is

$$\frac{x_{2i}^2}{x_{1i}} \hat{d}_{ri}.$$

From (12), we can get that

$$\hat{d}_{ri}(t) \equiv d_{ri}(t), \quad \forall\, t > T_1.$$

Based on the definition of $d_{ri}(t)$, it can be derived that

$$\frac{x_{2i}^2}{x_{1i}} \hat{d}_{ri} = a_{Tri}, \quad \forall\, t > T_1.$$

The target's tangential acceleration a_{Tri} is bounded by propulsion system limits and physical constraints, ensuring feasible maneuverability within practical engineering thresholds. Therefore, we can conclude that

$$\left|\frac{x_{2i}^2}{x_{1i}} \hat{d}_{ri}\right| \leq M,$$

where M is the upper bound of a_{Tri}. Furthermore, from the definition of the function tanh we can get

$$\left| k_5 \tanh\left(\operatorname{sig}^{\alpha_5}\left(\sum_{j=1}^{N} a_{ij}(t_{go,i} - t_{go,j}) \right)\right)\right| \leq k_5.$$

Therefore, from (33), we can derive that

$$\left| u_{ri} \right| \leq M + k_5.$$

Therefore, the FnTCG law proposed in this paper effectively avoids singularities while ensuring that the tangential acceleration along the LOS satisfies the input saturation constraints.

Remark 2. This work emphasizes the tangential acceleration constraint along the LOS direction, a critical yet often overlooked factor in terminal guidance. Unlike normal acceleration, which is governed by aerodynamic control surfaces with high maneuver bandwidth, tangential acceleration relies on thrust modulation — a process inherently bounded by propulsion system limits (e.g. maximum thrust and fuel flow rates). These constraints, distinct from normal overload capabilities, necessitate explicit saturation mechanisms to prevent unrealistic thrust demands and ensure energy-optimal engagement. The proposed guidance law addresses this by embedding a bounded saturation function for tangential acceleration commands, directly aligning with propulsion hardware limits while decoupling thrust dynamics from maneuver authority. This approach not only resolves singularity risks in conventional feedback-linearization-based methods but also bridges the gap between theoretical guidance designs and practical engineering constraints, where propulsion limitations dominate terminal-phase performance.

4. Numerical Simulation

To validate the effectiveness of the proposed FnTCG law, a numerical example was conducted, where four aircraft were employed to attack a maneuvering target. The parameters of the proposed finite-time extended state observer are designed as $\lambda_1 = 2.4, \lambda_2 = 1.5, \lambda_3 = 3.2, \lambda_4 = 1.6, \lambda_5 = 1.1, L = 100$. The guidance parameters are designed as follows:

$$\begin{cases} k_1 = 5, \quad k_2 = 10, \quad k_3 = 5, \quad k_4 = 10, \quad k_5 = 10, \\ \alpha_1 = 0.5, \quad \alpha_2 = 0.85, \quad \alpha_3 = 0.5, \\ \alpha_4 = 0.85, \quad \alpha_5 = 0.85. \end{cases}$$

The preset sequence of LOS angles are

$$\begin{cases} q_{\varepsilon d1} = 10, \quad q_{\varepsilon d2} = 5, \quad q_{\varepsilon d3} = -10, \\ q_{\varepsilon d1} = -5, \quad q_{\beta d1} = -10, \quad q_{\beta d2} = 5, \\ q_{\beta d3} = 10, \quad q_{\beta d1} = -5. \end{cases}$$

Figure 2 illustrates the communication topology among the aircraft, which is directed. Table 1 presents the initial conditions.

In Figs. 3 and 4, multiple aircraft successfully hit the maneuvering target, and the remaining flight time for the four aircraft achieves consensus after a certain time.

In Fig. 5, the elevation and azimuth LOS angles of multiple aircraft converge to the predetermined angle sequence after a certain time.

In Fig. 6, the angular rates of LOS angles for multiple aircraft stabilize at approximately zero after a certain time, which ensures an accurate target hit by the aircraft.

Figure 7 shows the acceleration commands in three directions for four aircraft, which indicates relatively smooth overload commands in multiple directions.

Figure 8 shows that the difference between the acceleration commands and the target's acceleration is strictly limited within the range of $(-10, 10)$, which is consistent with the design.

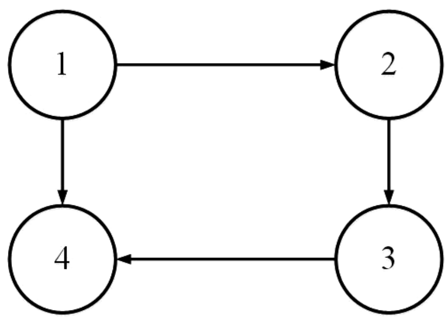

Fig. 2. Directed communication topology among four aircraft.

Table 1. Simulation initial conditions.

Aircraft	$r_i(0)$(m)	$\dot{r}_i(0)$(m/s)	$q_{si}(0)$ (°)	$\dot{q}_{si}(0)$ (°/s)	$q_{\beta i}(0)$ (°)	$\dot{q}_{\beta i}(0)$ (°/s)
1	10,000	−200	7	0	−5	0
2	9000	−180	2	0	3	0
3	11,000	−220	−8	0	2	0
4	12,000	−160	−5	0	−12	0

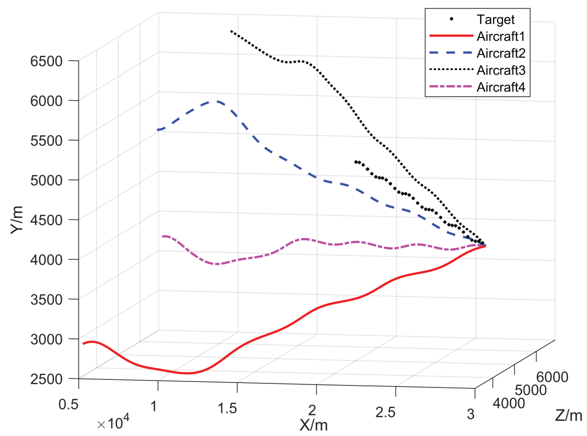

Fig. 3. Three-dimensional trajectories of four aircraft and a maneuvering target during the cooperative engagement phase.

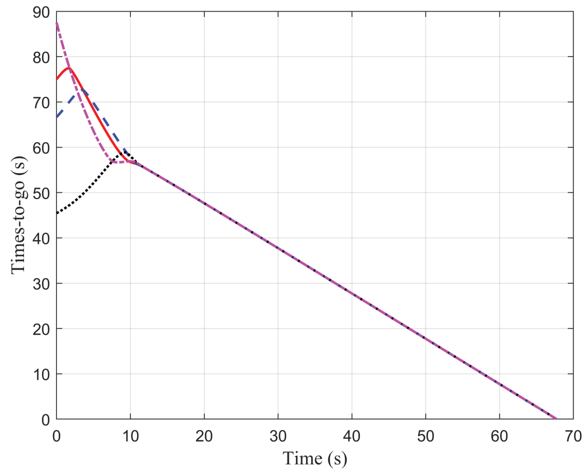

Fig. 4. Time-to-go for four aircraft.

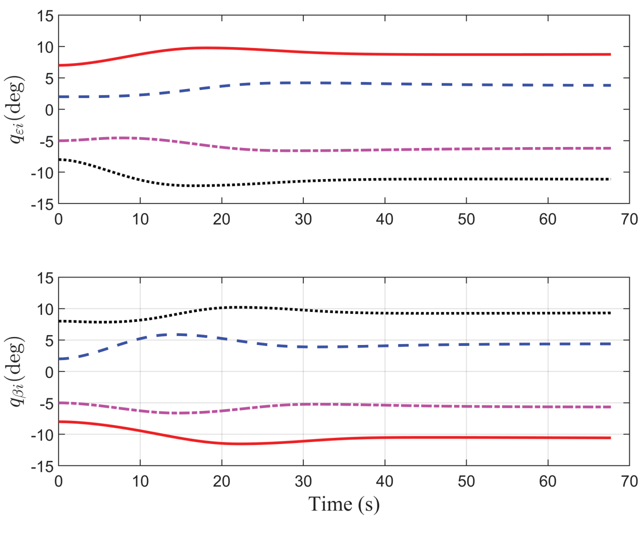

Fig. 5. LOS angles for four aircraft.

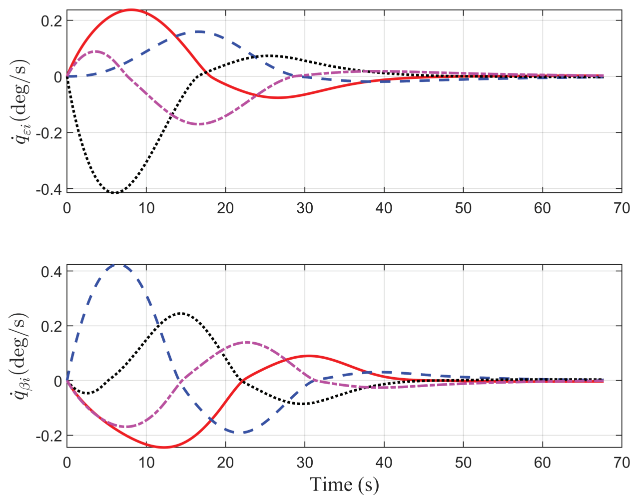

Fig. 6. LOS angle rates for four aircraft.

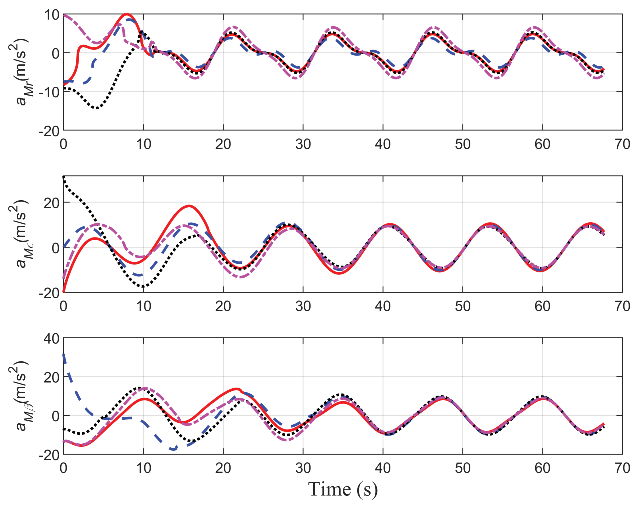

Fig. 7. Acceleration commands for four aircraft.

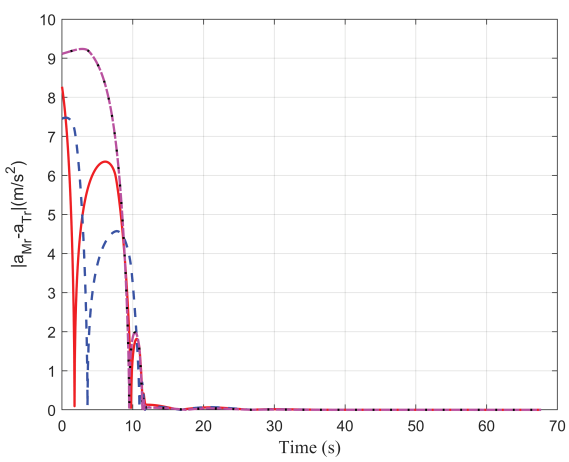

Fig. 8. Difference between acceleration commands and acceleration of the target.

To further demonstrate the advantages of the proposed 3D FnTCG law, the 3D fix-time cooperative guidance (FxTCG) law proposed in [28] is utilized to achieve the same cooperative mission as shown in Table 1. Reference [28] is a typical representative of the feedback linearization method. Due to its widespread application in cooperative guidance design, it holds significant representativeness. The parameters of the FxTCG law are selected according to [28] with the simulation results provided in Fig. 9.

By comparing the simulation results, it can be observed that although the FxTCG law can also achieve the terminal angle-constrained salvo attacks, the proposed FnTCG law presents three advantages over the approach in [28].

First, during the initial phase of guidance, the acceleration commands of the FnTCG law are significantly smaller. Specifically, the maximum acceleration commands for the FxTCG law in three directions are 44.1 m/s^2, 292.2 m/s^2 and 350.4 m/s^2, while those of the proposed FnTCG law are 14.2 m/s^2, 31.8 m/s^2 and 31.7 m/s^2, respectively. This discrepancy arises because the FxTCG law employs feedback linearization in its guidance design, multiplying the control variable by a linearization coefficient R, which is typically large in the initial stage, leading to excessively high acceleration commands.

Second, as illustrated in Fig. 9(d), the terminal tangential acceleration of the FxTCG law exhibits unexpected chattering, whereas the proposed FnTCG law does not. This difference is attributed to the singularity issues inherent in the guidance law of the comparative method at the terminal stage, which the proposed approach effectively mitigates.

Finally, the proposed FnTCG law demonstrates a shorter impact time. Simulation results indicate that the impact time for the FxTCG law is 71.1 s, while the impact time for the proposed guidance law is 67.3 s. This improvement is attributed

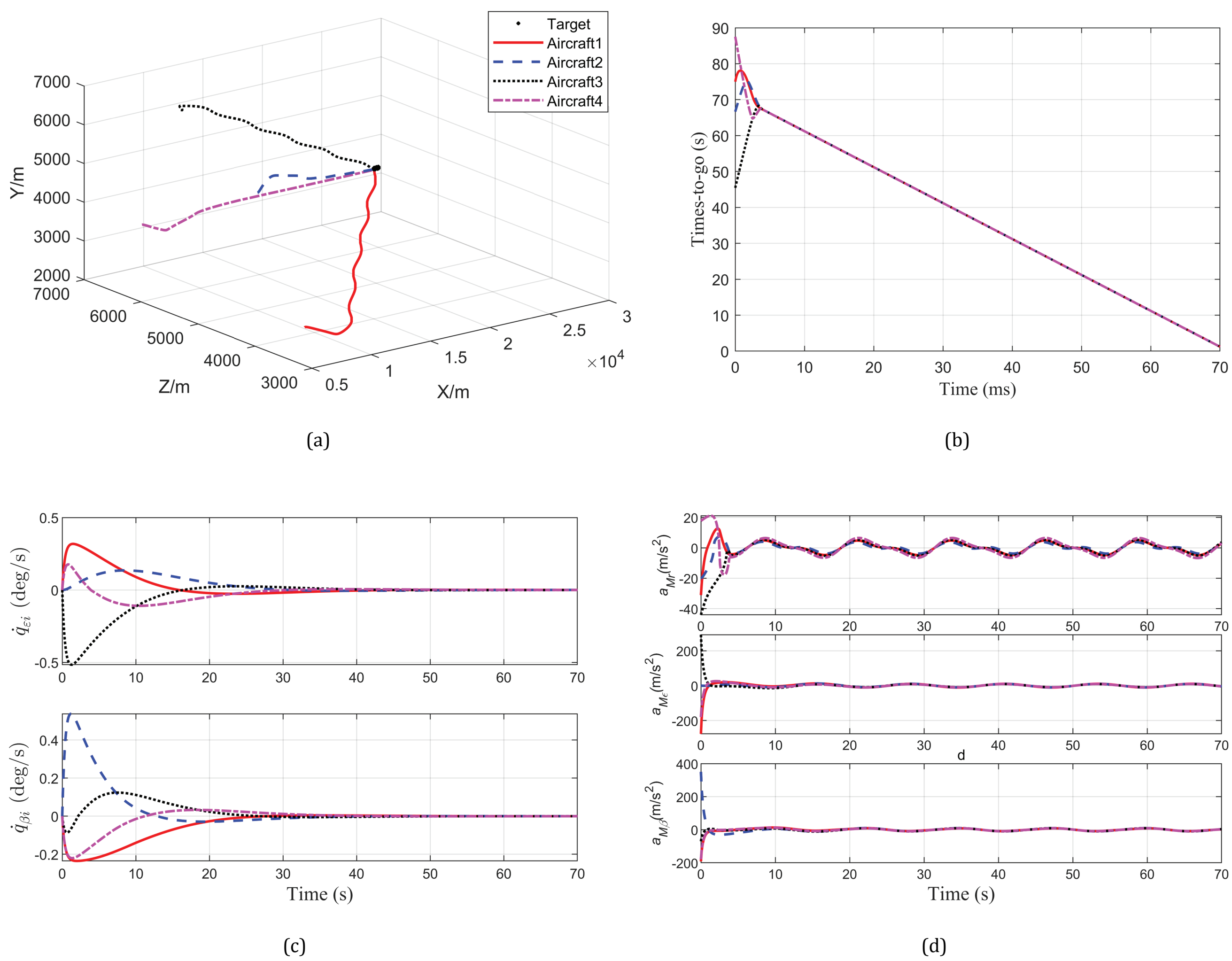

Fig. 9. Simulation results of the 3D FxTCG law.

to the avoidance of excessively large acceleration commands induced by feedback linearization, resulting in a smoother trajectory for the multiple aircraft and consequently reducing the time to impact the target.

5. Conclusion

This paper proposes a novel distributed cooperative guidance law, which achieves simultaneous attack on maneuvering targets. By designing cooperative guidance laws separately in LOS direction and LOS normal direction, simultaneous attack is achieved while satisfying the terminal LOS angle constraint. The design of the guidance laws avoids the additional control quantity introduced by feedback linearization and prevents the singularity problem of the guidance laws. A saturated nonlinear function is introduced in the LOS direction guidance law to satisfy the overload constraint in the LOS direction, which is beneficial for engineering applications. Additionally, the cooperative guidance laws designed in this paper meet the requirement of finite-time convergence, and the finite-time stability of the designed guidance laws is rigorously proved through theoretical analysis. Numerical simulations demonstrate the effectiveness of the designed distributed cooperative guidance law.

References

[1] I.-S. Jeon, J.-I. Lee and M.-J. Tahk, Impact-time-control guidance law for anti-ship missiles, *IEEE Trans. Control Syst. Technol.* **14**(2) (2006) 260–266.

[2] S. R. Kumar and D. Ghose, Sliding mode control based guidance law with impact time constraints, in *2013 American Control Conf.* (IEEE, 2013), pp. 5760–5765.

[3] S. Ghosh, D. Ghose and S. Raha, Three dimensional PN based impact angle control for higher speed nonmaneuvering targets, in *2013 American Control Conf.* (IEEE, 2013), pp. 31–36.

[4] L. Zhang, M. Sun, Z. Chen, Z. Wang and Y. Wang, Receding horizon trajectory optimization with terminal impact specifications, *Math. Probl. Eng.* **2014**(1) (2014) 604705.

[5] Y. Chen, J. Wang, C. Wang, J. Shan and M. Xin, Three-dimensional cooperative homing guidance law with field-of-view constraint, *J. Guid. Control Dyn.* **43**(2) (2020) 389–397.

[6] A. Sinha, S. R. Kumar and D. Mukherjee, Three-dimensional nonlinear cooperative salvo using event-triggered strategy, *J. Guid. Control Dyn.* **44**(2) (2021) 328–342.

[7] W. Dong, C. Wang, J. Wang and M. Xin, Three-dimensional nonsingular cooperative guidance law with different field-of-view constraints, *J. Guid. Control Dyn.* **44**(11) (2021) 2001–2015.

[8] C. Wang, W. Dong, J. Wang and M. Xin, Impact-angle-constrained cooperative guidance for salvo attack, *J. Guid. Control Dyn.* **45**(4) (2022) 684–703.

[9] Y. Zhang, S. Tang and J. Guo, Two-stage cooperative guidance strategy using a prescribed-time optimal consensus method, *Aerosp. Sci. Technol.* **100** (2020) 105641.

[10] V. Shaferman and T. Shima, Cooperative optimal guidance laws for imposing a relative intercept angle, *J. Guid. Control Dyn.* **38**(8) (2015) 1395–1408.

[11] V. Shaferman and T. Shima, Cooperative differential games guidance laws for imposing a relative intercept angle, *J. Guid. Control Dyn.* **40**(10) (2017) 2465–2480.

[12] M. Nikusokhan and H. Nobahari, Closed-form optimal cooperative guidance law against random step maneuver, *IEEE Trans. Aerosp. Electron. Syst.* **52**(1) (2016) 319–336.

[13] J. Zhao, R. Zhou and Z. Dong, Three-dimensional cooperative guidance laws against stationary and maneuvering targets, *Chin. J. Aeronaut.* **28**(4) (2015) 1104–1120.

[14] J. Zhao and R. Zhou, Unified approach to cooperative guidance laws against stationary and maneuvering targets, *Nonlinear Dyn.* **81** (2015) 1635–1647.

[15] Q. Zhao, X. Dong, X. Song and Z. Ren, Cooperative time-varying formation guidance for leader-following missiles to intercept a maneuvering target with switching topologies, *Nonlinear Dyn.* **95** (2019) 129–141.

[16] X. H. Wang and C. P. Tan, 3-D impact angle constrained distributed cooperative guidance for maneuvering targets without angular-rate measurements, *Control Eng. Pract.* **78** (2018) 142–159.

[17] F. Liu, X. Dong, Q. Li and Z. Ren, Robust multi-agent differential games with application to cooperative guidance, *Aerosp. Sci. Technol.* **111** (2021) 106568.

[18] S. Zhai, X. Wei and J. Yang, Cooperative guidance law based on time-varying terminal sliding mode for maneuvering target with unknown uncertainty in simultaneous attack, *J. Franklin Inst.* **357**(16) (2020) 11914–11938.

[19] Z. Wang, W. Fu, Y. Fang, S. Zhu, Z. Wu and M. Wang, Prescribed-time cooperative guidance law against maneuvering target based on leader-following strategy, *ISA Trans.* **129** (2022) 257–270.

[20] J. Yu, X. Dong, Q. Li and Z. Ren, Distributed cooperative encirclement hunting guidance for multiple flight vehicles system, *Aerosp. Sci. Technol.* **95** (2019) 105475.

[21] J. Yu, X. Dong, Q. Li, J. Lv and Z. Ren, Distributed adaptive cooperative time-varying formation tracking guidance for multiple aerial vehicles system, *Aerosp. Sci. Technol.* **117** (2021) 106925.

[22] H. You, X. Chang, J. Zhao, S. Wang and Y. Zhang, Three-dimensional impact-angle-constrained cooperative guidance strategy against maneuvering target, *ISA Trans.* **138** (2023) 262–280.

[23] J. Song, S. Song and S. Xu, Three-dimensional cooperative guidance law for multiple missiles with finite-time convergence, *Aerosp. Sci. Technol.* **67** (2017) 193–205.

[24] L. Jing, L. Zhang, J. Guo and N. Cui, Fixed-time cooperative guidance law with angle constraint for multiple missiles against maneuvering target, *IEEE Access* **8** (2020) 73268–73277.

[25] S. Liu, B. Yan, T. Zhang, P. Dai, R. Liu and J. Yan, Three-dimensional cooperative guidance law for intercepting hypersonic targets, *Aerosp. Sci. Technol.* **129** (2022) 107815.

[26] Z. Chen, W. Chen, X. Liu and J. Cheng, Three-dimensional fixed-time robust cooperative guidance law for simultaneous attack with impact angle constraint, *Aerosp. Sci. Technol.* **110** (2021) 106523.

[27] P. Zhang and X. Zhang, Multiple missiles fixed-time cooperative guidance without measuring radial velocity for maneuvering targets interception, *ISA Trans.* **126** (2022) 388–397.

[28] W. Dong, C. Wang, J. Wang, Z. Zuo and J. Shan, Fixed-time terminal angle-constrained cooperative guidance law against maneuvering target, *IEEE Trans. Aerosp. Electron. Syst.* **58**(2) (2021) 1352–1366.

[29] S. Xu, X. Song and C. Li, Cooperative guidance law with maneuverability awareness: A decentralized solution, *Chin. J. Aeronaut.* **37**(7) (2024) 450–457.

[30] F. Dong, X. Zhang and P. Tan, Non-singular terminal sliding mode cooperative guidance law under impact angle constraint, *J. Franklin Inst.* **361**(14) (2024) 107079.

[31] W. Ren and R. W. Beard, Consensus seeking in multiagent systems under dynamically changing interaction topologies, *IEEE Trans. Autom. Control* **50**(5) (2005) 655–661.
[32] Y. Hong, Y. Xu and J. Huang, Finite-time control for robot manipulators, *Syst. Control Lett.* **46**(4) (2002) 243–253.
[33] A. Levant, Higher-order sliding modes, differentiation and output-feedback control, *Int. J. Control* **76**(9–10) (2003) 924–941.
[34] H. Khalil, *Nonlinear Systems* (Prentice Hall, 2002).
[35] S. P. Bhat and D. S. Bernstein, Continuous finite-time stabilization of the translational and rotational double integrators, *IEEE Trans. Autom. Control* **43**(5) (1998) 678–682.